the FEBS Journal

Carboxylate and aromatic active-site residues are determinants of high-affinity binding of ω-aminoaldehydes to plant aminoaldehyde dehydrogenases

David Kopečný[1], Martina Tylichová[1], Jacques Snegaroff[2], Hana Popelková[3] and Marek Šebela[1]

1 Department of Protein Biochemistry and Proteomics, Centre of the Region Haná for Biotechnological and Agricultural Research, Faculty of Science, Palacký University, Olomouc, Czech Republic
2 Institut Jean-Pierre Bourgin, UMR1318 INRA-AgroParisTech, Versailles Cedex, France
3 Department of Molecular, Cellular and Developmental Biology, University of Michigan, Ann Arbor, MI, USA

Keywords
3-aminopropionaldehyde; 4-aminobutyraldehyde; 4-guanidinobutyraldehyde; aminoaldehyde dehydrogenase; betaine aldehyde

Correspondence
D. Kopečný & M. Šebela, Department of Protein Biochemistry and Proteomics, Center of the Region Haná for Biotechnological and Agricultural Research, Faculty of Science, Palacký University, Šlechtitelů 11, CZ-783 71 Olomouc, Czech Republic
Fax: +420 585634933
Tel: +420 585634927
E-mail: kopecny_david@yahoo.co.uk; marek.sebela@upol.cz

(Received 23 May 2011, revised 7 June 2011, accepted 6 July 2011)

doi:10.1111/j.1742-4658.2011.08239.x

The crystal structures of both isoforms of the aminoaldehyde dehydrogenase from pea (PsAMADH) have been solved recently [Tylichová *et al.* (2010) *J Mol Biol* **396**, 870–882]. The characterization of the PsAMADH2 proteins, altered here by site-directed mutagenesis, suggests that the D110 and D113 residues at the entrance to the substrate channel are required for high-affinity binding of ω-aminoaldehydes to PsAMADH2 and for enzyme activity, whereas N162, near catalytic C294, contributes mainly to the enzyme's catalytic rate. Inside the substrate cavity, W170 and Y163, and, to a certain extent, L166 and M167 probably preserve the optimal overall geometry of the substrate channel that allows for the appropriate orientation of the substrate. Unconserved W288 appears to affect the affinity of the enzyme for the substrate amino group through control of the substrate channel diameter without affecting the reaction rate. Therefore, W288 may be a key determinant of the differences in substrate specificity found among plant AMADH isoforms when they interact with naturally occurring substrates such as 3-aminopropionaldehyde and 4-aminobutyraldehyde.

Introduction

Polyamine breakdown has attracted increasing attention in recent years because of its association with programmed cell death processes under normal physiological conditions and during stress responses [1]. This oxidative pathway is mediated by amine oxidases, and produces various ω-aminoaldehydes, such as 3-aminopropionaldehyde (APAL) and 4-aminobutyraldehyde (ABAL) [2]. The free polyamine-derived aminoaldehydes, especially APAL, are reactive and cytotoxic when present at high concentrations [3]. Their oxidation by the $NAD(P)^+$-dependent aminoaldehyde dehydrogenase (AMADH) results in the formation of nontoxic metabolites, such as β-alanine and γ-aminobutyric acid [4].

AMADH enzymes belong to the aldehyde dehydrogenase families 9 and 10 (ALDH9 and ALDH10) [5].

Abbreviations
ABAL, 4-aminobutyraldehyde; ALDH, aldehyde dehydrogenase; AMADH, aminoaldehyde dehydrogenase; APAL, 3-aminopropionaldehyde; BAL, betaine aldehyde; GBAL, 4-guanidinobutyraldehyde; GPAL, 3-guanidinopropionaldehyde; PsAMADH, aminoaldehyde dehydrogenase from pea; TMABAL, *N,N,N*-trimethyl-4-aminobutyraldehyde; TMAPAL, *N,N,N*-trimethyl-3-aminopropionaldehyde.

In the past, the enzyme was frequently referred to as 4-aminobutyraldehyde dehydrogenase (ABALDH, EC 1.2.1.19) and 4-guanidinobutyraldehyde dehydrogenase (GBALDH, EC 1.2.1.54), which are related to polyamine metabolism, but also as the betaine aldehyde dehydrogenase (BADH, EC 1.2.1.8) and the 4-trimethylaminobutyraldehyde dehydrogenase (TMABALDH, EC 1.2.1.47) (Fig. 1). Recently, a loss of AMADH activity was found to be associated with the characteristic fragrance of several rice varieties, such as jasmine and basmati [6,7]. Since that time, the study of the physiological aspects of plant AMADHs has become attractive for economic reasons. Although substrate specificity can vary among species, all of the enzymes mentioned above should be classified as AMADHs.

The reaction of AMADHs, as of other ALDHs, involves a nucleophilic attack by the catalytic cysteine on the aldehyde substrate, followed by thioester formation and hydride transfer to the $NAD(P)^+$ coenzyme [8]. The product acid is then released by hydrolysis with the participation of a conserved glutamate acting as an active-site base. Several studies have evaluated the importance of the active-site residues in the ALDH superfamily. The catalytic cysteine [C294 in pea (*Pisum sativum*) PsAMADH2 numbering] has been mutated in rat liver ALDH2 and human ALDH2 [9,10]. Its replacement with alanine resulted in a complete loss of activity, whereas its mutation to serine, as a poor nucleophile, resulted in a 10^2–10^5-fold lower dehydrogenase activity. The role of the active-site base (E260 in PsAMADH2) has been studied in detail in human ALDH2 and ALDH3 [11,12]. For ALDH2, it has been shown that mutations to glutamine or aspartate cause a 10^2–10^3-fold lower activity, whereas, in ALDH3, the same replacements of E260 completely abolish the activity.

In plants, AMADHs form dimers. The crystal structures of the two AMADH isoenzymes from pea (*P. sativum*) have been reported recently [4]. The structural analysis of both PsAMADHs revealed that the entrance to the 14-Å-long substrate channel in each subunit is formed by the residues W109, D113, P452 and C453 (Fig. 2), whereas the interior is formed by D110, N162, Y163, L166, M167, W170, E260, F284, W288, I293, C294, S295, Q451 and W459. The presence of both carboxylate and aromatic residues at the entrance to the substrate channel is typical for all plant AMADHs, and almost all of the residues in the substrate channel are evolutionarily highly conserved, except for W288 and W109. The latter residues, together with D113 in PsAMADH1 and PsAMADH2, have been proposed to interact with the substrate amino group [4].

Plant AMADHs bind various aminoaldehydes with high affinity. This characteristic distinguishes the AMADH family from other ALDH families, such as ALDH2 and ALDH3, which are able to oxidize a broad spectrum of aliphatic and aromatic aldehydes. The recently reported biochemical and crystallographic study on the structure and function of AMADHs from pea [4] allowed an assessment of the residues in the substrate channel that may be important for high-affinity binding of this enzyme to aminoaldehydes. Both the variable and conserved active-site residues were proposed to interact with natural substrates. This work uses site-directed mutagenesis of PsAMADH2

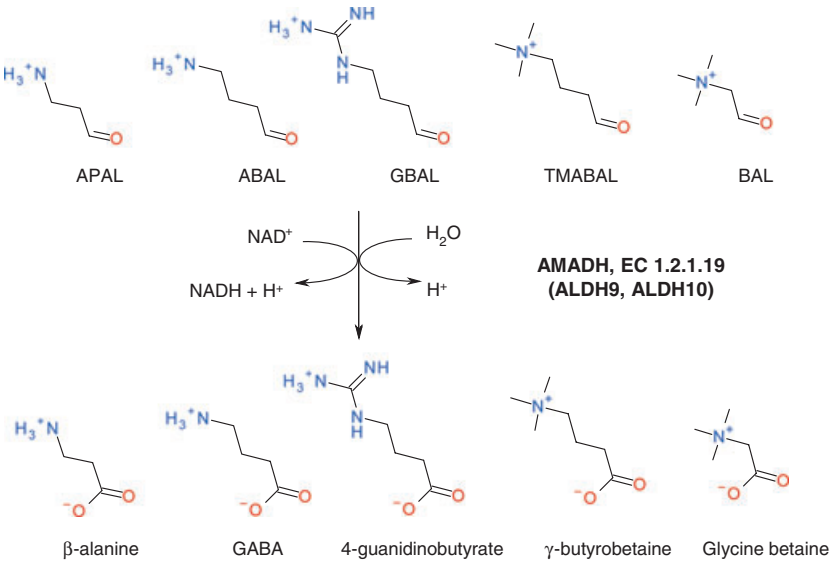

Fig. 1. Natural substrates of aminoaldehyde dehydrogenases (AMADHs) [enzymes from the aldehyde dehydrogenase (ALDH) families 9 and 10]. 3-Aminopropionaldehyde (APAL) is converted to β-alanine, 4-aminobutyraldehyde (ABAL) to γ-aminobutyric acid (GABA), 4-guanidinobutyraldehyde (GBAL) to 4-guanidinobutyric acid, *N,N,N*-trimethyl-4-aminobutyraldehyde (TMABAL) to γ-butyrobetaine and betaine aldehyde (BAL) to glycine betaine.

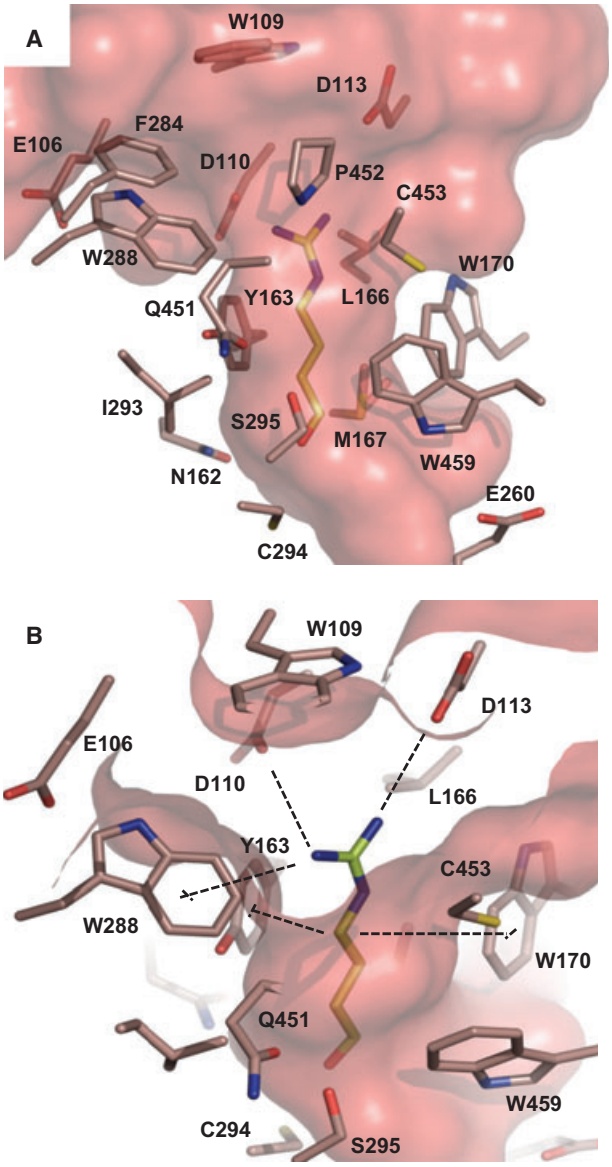

Fig. 2. The active site of pea AMADH2. (A) The substrate channel of PsAMADH2 (PDB 3IWJ) with neighboring residues. The total surface of the channel (shown in red) was calculated using HOLLOW [13] with a grid spacing of 0.8 Å and an interior probe of 1.1 Å. A model of the 4-guanidinobutyraldehyde (GBAL) substrate (in yellow) is shown for illustration. (B) The residues that are essential for the interaction of the enzyme with the substrate's terminal amino group and residues located at a distance of 3.5–4 Å from the closest atom of the GBAL model molecule are indicated by broken lines.

and analyzes the resulting mutated proteins in order to find structural clues to the substrate specificity of AMADH. The results reported here show that various mutated PsAMADH2 proteins exhibit different affinity for ω-aminoaldehydes, and that the nitrogen atom of the substrate interacts with both acidic and aromatic amino acid residues of PsAMADH2, indicating that the process of substrate binding is very complex in AMADH.

Results and Discussion

Mutagenesis of carboxylate amino acid residues at the entrance to the substrate channel of PsAMADH2

An earlier study on polyamine binding showed that the PotD and PotF receptors of a bacterial polyamine transport system bind the polyamine substrates spermidine and putrescine through carboxylate residues. Specifically, ionic interactions anchor the protonated amino group of polyamines to carboxylate residues in the substrate-binding site of the protein [14,15]. In plant polyamine oxidases, the substrate-binding carboxylate residues aspartic acid and glutamic acid form a carboxylate ring that is located on the surface of the enzyme, and functions to guide the positively charged polyamine substrates into the catalytic tunnel [16]. This is consistent with a previous study that employed chemical modification of native PsAMADH1 [17], and showed a possible key role of carboxylate residues for AMADH activity. In this aspect, the entrance to the AMADH substrate channel resembles that of plant polyamine oxidases.

Based on the acido-basic nature of carboxylate residues, it has been assumed that the protonated substrate nitrogen electrostatically interacts with the highly conserved negatively charged residues in the active site of PsAMADH2. To examine this assumption, mutated PsAMADH2 proteins with altered E106, D110 and D113 were produced. In addition to single mutations, the double mutant D110A + D113A and the triple mutant E106A + D110A + D113A were also constructed to study the possible cumulative effect of the mutations. The production of mutated proteins was verified using SDS/PAGE (Fig. 3A), and their function was probed using activity assays with APAL and ABAL (Table 1). To verify that none of the functional changes observed here was caused by significant alterations in the solution structures of the mutated proteins relative to that of the recombinant wild-type (WT), CD spectroscopy was used in this study. Figure 3B shows that the far-UV CD spectra for all of the PsAMADH2 variants are very similar to the far-UV CD spectrum of WT PsAMADH2; the differences in the measured curves, normalized to the mean residual ellipticity maximum at 208 nm, do not exceed 3% in the interval 208–225 nm. Moreover, the calculated secondary

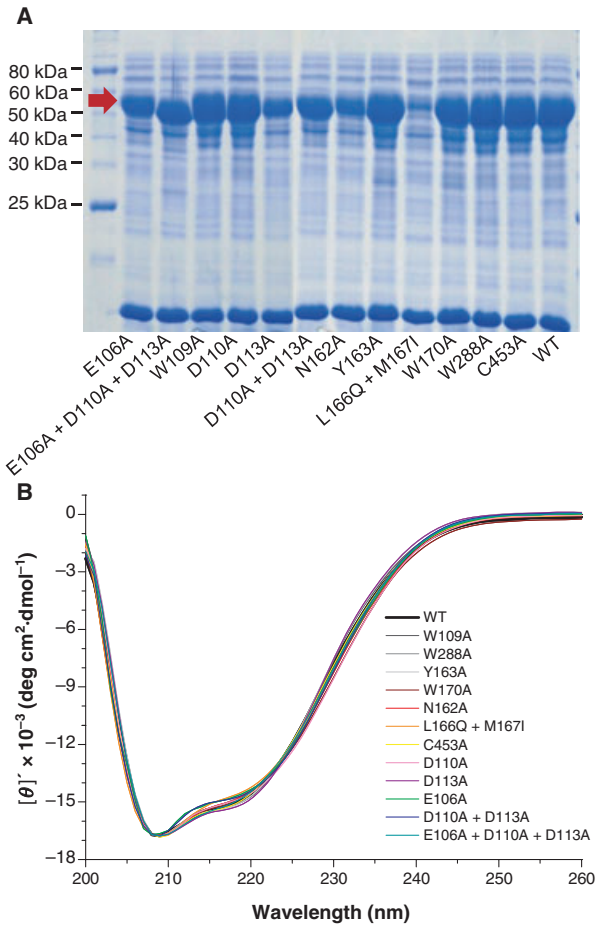

Fig. 3. (A) Bio-Safe Coomassie Blue-stained SDS/PAGE gels of *Escherichia coli* cell lysates containing the wild-type (WT) and mutated PsAMADH2 proteins (10 μL were loaded in each lane). The red arrow indicates the migration of the produced enzyme (~ 55 kDa). (B) Far-UV CD spectra of purified WT and mutated PsAMADH2 (0.5 mg·mL^{-1}) in 20 mM Tris/HCl buffer, pH 9.0. The spectra were normalized to the maximum of the mean residual ellipticity at 208 nm.

structural elements (~ 40% of α-helices and ~ 15% of β-sheets), based on the spectra in Fig. 3B, coincide well with the estimates obtained from the crystal structure of the WT enzyme [4]. Taken together with the fact that the catalytic activity of PsAMADH2 is associated with the dimeric structure, and any dissociation of this dimer into individual subunits appears to be incompatible with the catalytic function of enzymes within the entire ALDH superfamily [4], the data in Fig. 3B indicate that all of the mutated proteins retain protein folding in solution that is very similar to that of WT PsAMADH2, and thus the mutations to the PsAMADH2 active site reported here do not induce substantial conformational changes in the overall structure of PsAMADH2.

Table 1. Kinetic parameters of pea AMADH2 proteins with the natural substrates 3-aminopropionaldehyde (APAL) and 4-aminobutyraldehyde (ABAL). The activities were measured in 0.15 M Tris/HCl buffer, pH 9.0. Kinetic constants were measured using a saturating NAD$^+$ concentration of 500 μM. All K_m and V_{max} values are given in μM and nmol·s^{-1}·mg^{-1}, respectively. The values for wild-type (WT) PsAMADH2 [4] are shown for comparison.

	APAL		ABAL	
Enzyme	K_m	V_{max}	K_m	V_{max}
WT PsAMADH2	10	190	29	57
E106A	31	72	50	33
E106A + D110A + D113A	–	0.02	–	0.03
W109A	12	180	32	55
D110A	375	49	890	25
D113A	260	121	575	21
D110A + D113A	480	1.9	1100	0.6
N162A	220	0.8	66	0.3
Y163A	1190	9.5	820	23
L166Q + M167I	55	49	120	25
W170A	31	69	250	4
W288A	35	185	61	60
C453A	14	188	34	61

The data presented in Table 1 show that the E106A mutation leads to a slight increase in K_m and decrease in V_{max}. As the crystal structure of PsAMADH2 [4] shows that the E106 carboxylate group is hydrogen bonded to the protein backbone in the vicinity of W288, E106 cannot, in principle, interact with the substrate nitrogen. The data in Table 1 can rather be interpreted to indicate that the impaired affinity of E106A for a substrate is a result of an effect of E106 on W288, a residue that was found to be involved in substrate binding by PsAMADH2 (see Mutagenesis of aromatic amino acid residues in the PsAMADH2 substrate channel section).

Alterations of the negatively charged residues D110 and D113 result in D110A and D113A proteins with significantly altered kinetic parameters (Table 1 and Fig. 4); the K_m values are 25–35 times higher and the V_{max} values are two to three times lower than those for WT. A more profound effect on PsAMADH2 activity is observed with the double mutant D110A + D113A. This mutated protein has a 100-fold lower turnover and almost a 50-fold higher K_m (Table 1) relative to WT. These results suggest that D110 and D113 clearly recognize the protonated substrate nitrogen. Although the presence of E/D110 is a typical structural feature of almost all plant ALDHs, D113 is not conserved; some of the members of the ALDH2 and ALDH3 families possess a nonpolar residue at this position. Therefore, the presence of both aspartic residues D110 and D113 is not only essential to maintain the high affinity of PsA-

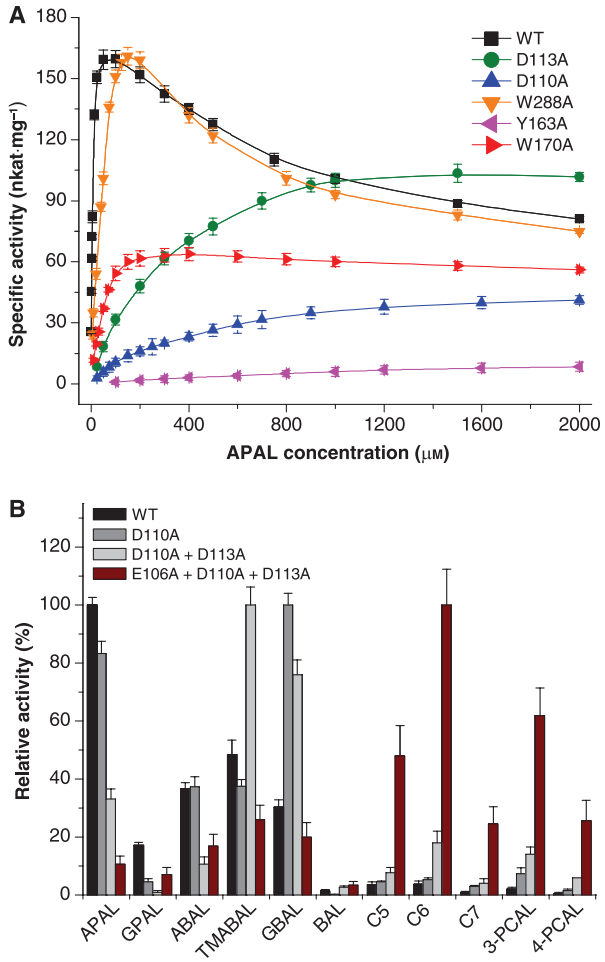

Fig. 4. (A) Saturation curves of activity for wild-type (WT) PsAMADH2 and selected mutated variants measured with 3-aminopropionaldehyde (APAL) as a substrate in the presence of 500 μM NAD^+. (B) A comparison of the substrate specificity of WT PsAMADH2 and the D110A, D110A + D113A and E106 + D110A + D113A proteins measured with 1 mM of substrate. The specific activities of PsAMADH2 variants with 1 mM APAL were as follows: 101 nkat·mg^{-1} for WT, 36 nkat·mg^{-1} for D110A, 1.2 nkat·mg^{-1} for D110A + D113A and 0.02 nkat·mg^{-1} for E106A + D110A + D113A. ABAL, 4-aminobutyraldehyde; APAL, 3-aminopropionaldehyde; BAL, betaine aldehyde; C5, valeraldehyde; C6, capronaldehyde; C7, enanthaldehyde; GBAL, 4-guanidinobutyraldehyde; GPAL, 3-guanidinopropionaldehyde; PCAL, pyridine carboxaldehyde; TMABAL, *N,N,N*-trimethyl-4-aminobutyraldehyde.

MADH2 for aminoaldehydes, it is also needed to maintain the rate of its oxidation reaction. As the activity of the mutated proteins with ω-aminoaldehydes decreases, the relative reaction rates with 3- and 4-pyridine carboxaldehydes and with *n*-alkyl aldehydes (particularly with capronaldehyde) increase. This is especially true for the triple mutant E106A + D110A + D113A, which exhibits a specific activity four orders of magnitude lower than WT, and capronaldehyde is its best substrate (Fig. 4). These results suggest that, with the E106A + D110A + D113A mutation, the enzyme becomes a nonspecific ALDH.

Finally, it should be noted that the activity of WT PsAMADH2 is inhibited by an excess APAL concentration in the reaction mixture (see Fig. 4A). A similar inhibitory effect is also observed with *N,N,N*-trimethyl-4-aminobutyraldehyde (TMABAL) and 4-guanidinobutyraldehyde (GBAL) (data not shown). This is a typical AMADH feature that disappears when the catalytic function of the enzyme is impaired. The D113A and D110A proteins exhibit very little or no signs of substrate inhibition. The mechanism of this inhibitory process in AMADH is unclear. One possible hypothesis may be that two substrate molecules can enter the optimally shaped substrate channel at the same time and bind to the carboxylate pair D110 and D113 at its surface, but only one can be present in a position enabling direct access to the catalytic cysteine C294. The catalytic cysteine (pK_a = 8.0) [17] exists in its thiolate form at pH values significantly > 8.0, which facilitates efficient nucleophilic attack on a substrate. The kinetic analysis presented here was performed at pH 9.0 in order to maintain the majority of APAL and ABAL molecules protonated [$pK_{a(APAL)}$ ~9.3, $pK_{a(ABAL)}$ ~ 9.8, $pK_{a(GBAL)}$ > 12) [3,18] and, at the same time, to allow for sufficient catalytic rates. The results from the activity measurements at various pH values (Fig. S4) provide evidence that the enzyme exhibits both a high affinity to APAL and strong substrate inhibition at pH ≤ 9.4. However, at pH values of 9.6 and greater, the K_m values for APAL increase in accord with substrate deprotonation, whereas the inhibitory effect of the substrate disappears and the reaction with APAL follows Michaelis–Menten kinetics.

Mutagenesis of aromatic amino acid residues in the PsAMADH2 substrate channel

The entrance of the substrate channel in plant polyamine oxidases is lined by several aromatic amino acid residues [16]. Figure 2 shows that PsAMADH2 resembles polyamine oxidases in this respect. Based on the PsAMADH2 crystal structure [4], a π-electron stacking interaction between an entering substrate and surrounding aromatic residues of PsAMADH2 can be expected. This hypothesis was examined using mutations in the highly conserved Y163 and W170 residues and in the less conserved W109 and W288 residues of PsAMADH2, all of which were mutated to alanine.

The W109 residue separates the upper funnel-shaped domain of the channel into two halves, and therefore

was expected to function as a gate to the substrate channel (Fig. 2B). This hypothesis proved to be invalid, as the W109A mutation does not cause any changes in substrate specificity, affinity and activity with common substrates, except for GBAL (Table 1, Fig. 5). This substrate possesses the longest chain of all compounds tested here, and its oxidation is slightly affected by the W109A mutation. Thus, the data shown here suggest that W109 plays only a minor role in the binding of the substrate amino group, which is consistent with the fact that ~ 50% of all known AMADH sequences have glycine, alanine, serine or leucine at the homologous position.

In comparison with W109A, the W288A protein exhibits a more distinct behavior. It catalyzes the conversion of APAL and ABAL with a near-WT level of activity, but exhibits doubled reaction rates with GBAL and TMABAL (Table 1, Figs 4 and 5). It suggests that the W288 residue binds the substrate nitrogen, as deduced from the crystal structures of PsAMADH1 and PsAMADH2 [4]. The affinity of W288A for APAL and ABAL is decreased, which is evidenced by two- to three-fold higher K_m values relative to WT PsAMADH2 (Table 1). This result indicates that the substrate channel diameter may be enlarged and that the π-electron stacking interaction with the electrophilic protonated amino group of the substrate may be weakened in W288A. This interpretation is in agreement with the kinetic properties of PsAMADH1 [4], which carries phenylalanine in place of tryptophan at the homologous position. It has been shown that the presence of F288 in PsAMADH1 slightly widens the substrate channel relative to that in PsAMADH2, and that WT PsAMADH1 exhibits higher K_m values for APAL and ABAL than does WT PsAMADH2 [4]. These higher K_m values of PsAMADH1 for the substrate are comparable with those of W288A PsAMADH2 (Table 1) [4]. Finally, it is notable that the W109A and W288A variants exhibit substrate inhibition with APAL, in contrast with the results obtained with alanine mutations in the D110 and D113 residues, which also line the substrate channel of PsAMADH2 (see Figs 2 and 4A). This could confirm the hypothesis mentioned above that the interaction between an appropriately oriented protonated substrate and the carboxylate groups of D110 and/or D113 may be responsible for the inhibitory effect with an excess of APAL (or other protonated aminoaldehyde).

The two highly conserved aromatic residues, Y163 and W170, appear to have an important function in PsAMADH2. The data presented in Table 1 and Figs 4 and 5 show that the Y163A protein exhibits a substantial decline in V_{max} and a significant increase in

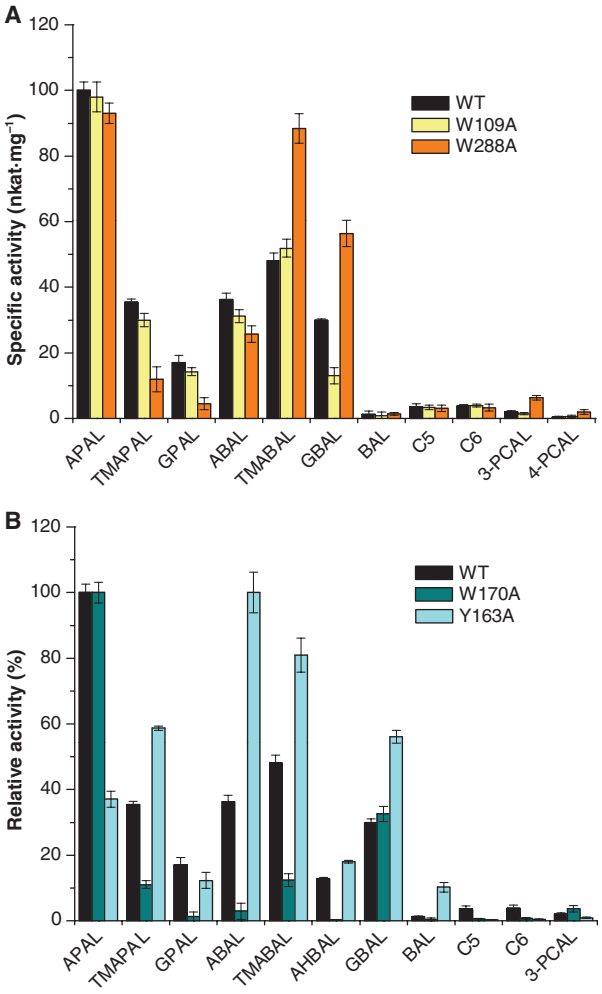

Fig. 5. Substrate specificity for wild-type (WT) PsAMADH2 and the W109A and W288A proteins (A) and for WT PsAMADH2 and the W170A and Y163A proteins (B) measured with 1 mM of substrate. The specific activities of PsAMADH2 variants with 1 mM 3-aminopropionaldehyde (APAL) were as follows: 101 nkat·mg^{-1} for WT, 6 nkat·mg^{-1} for Y163A, 62 nkat·mg^{-1} for W170A, 98 nkat·mg^{-1} for W109A and 93 nkat·mg^{-1} for W288A. ABAL, 4-aminobutyraldehyde; AHBAL, 4-amino-2-hydroxybutyraldehyde; APAL, 3-aminopropionaldehyde; BAL, betaine aldehyde; C5, valeraldehyde; C6, capronaldehyde; GBAL, 4-guanidinobutyraldehyde; GPAL, 3-guanidinopropionaldehyde; PCAL, pyridine carboxaldehyde; TMABAL, *N,N,N*-trimethyl-4-aminobutyraldehyde; TMAPAL, *N,N,N*-trimethyl-3-aminopropionaldehyde.

K_m, and that APAL is a weaker substrate for this enzyme than are ABAL, TMABAL and GBAL. In fact, this mutated protein is unique, because it is the only mutated protein presented here for which the oxidation of APAL is less efficient than the conversion of ABAL; APAL is generally the most preferred substrate for plant AMADHs. The very high K_m values indicate the important role of the hydrogen bonding interaction

between the hydroxyl of Y163 and the amino group of the substrate. In contrast, the W170A mutation impairs mainly the oxidation rate of PsAMADH2 with ABAL, which is only ~ 5% of the rate observed with APAL as a substrate. None of these mutated variants shows any activity with *n*-alkyl aldehydes. Both aromatic residues Y163 and W170 constitute the middle section of the substrate channel, and are only ~ 3.5 Å apart from the substrate's C3 and C4 atoms when it binds in the active site (Fig. 2B). Thus, the results in Table 1 and Figs 4 and 5 indicate that the substrate channel becomes enlarged as a result of the W → A and Y → A mutations. The D110 residue is located just above Y163, and is reachable by C4 aminoaldehydes. Thus, in Y163A, it is possible that D110 may partially substitute for the function of Y163. However, there is no such residue near W170 that could substitute its function in the W170A protein, which is consistent with the more significant decrease in its V_{max} value. Both the Y163 and W170 aromatic side-chains anchor the carbon chain of the substrates through van der Waals' interactions, which is in agreement with the observed inability of the Y163A and W170A proteins to oxidize *n*-alkyl aldehydes. Taken together, the data shown here suggest that Y163 and W170 in PsAMADH2 are necessary to maintain the overall geometry of the active site that allows for the binding of the substrate molecule in an appropriate orientation towards the catalytic cysteine C294, which results in the optimal reaction rate. In contrast, the near-WT rate of activity observed here for W109A and W288A suggests that the substrate position towards catalytic C294 remains unaffected by W109 → A and W288 → A replacements.

Mutagenesis of various amino acid residues inside the substrate cavity of PsAMADH2

The amino acid residue pairing of L166 and M167 residues in the interior of the substrate channel (Fig. 2), and is conserved in all known plant AMADH sequences; the AMADH enzymes from fish and animals contain a Q–I pair instead. To examine the importance of leucine and methionine in the active site of plant AMADHs, the double mutant L166Q + M167I of PsAMADH2 was produced (Fig. 3A). This mutated protein consistently exhibits a lower expression yield relative to the other PsAMADH2 variants presented here. Far-UV CD spectroscopy (Fig. 3B) did not reveal any significant changes in the secondary structure of L166Q + M167I relative to that of WT PsAMADH2 that would indicate an altered solution structure and proteolysis of this variant. Therefore, it is difficult to elucidate the exact origin of this phenomenon, as the production of this particular plant protein in *Escherichia coli* can interfere with the bacterial protein expression mechanism in various phases. The functional characterization in Table 1 shows that the L166Q + M167I double mutation causes a slight increase in K_m values, together with a reduction in V_{max}. The mutated enzyme oxidizes 4-pyridine carboxaldehyde with a relative rate of 6% compared with the rate with APAL, but does not show any activity with *n*-alkyl aldehydes (data not shown). Consistent with the results obtained here on the Y163A and W170A variants of PsAMADH2, both L166 and M167 also appear to play a role in preserving the geometry of the PsAMADH2 active site.

In the PsAMADH2 crystal structure [4], the substrate channel also contains the C453 residue that resides near the L166–M167 pair and in proximity to W170 (Fig. 2). Given the role of W170 in PsAMADH2 activity (see the previous section), it has been hypothesized that this cysteine could be involved in substrate binding. The characterization of the C453A variant of PsAMADH2 (Table 1), however, reveals that the replacement of C453 with alanine does not cause any changes in substrate specificity, affinity and activity, indicating that the role of C453 in substrate binding is negligible.

Highly conserved N162, the third amino acid residue in the consensus PW*N*YP motif of PsAMADH2, resides deep inside the substrate channel. The side-chain amide nitrogen of N162 and the NH group of catalytic C294 appear at distances of ~ 3.2 and ~ 2.7 Å, respectively, from the model-built substrate oxygen atom or from the glycerol oxygen atom mimicking the bound substrate in both PsAMADHs [4]. These two nitrogen atoms have been proposed to form an oxyanion hole that stabilizes the thiohemiacetal and thioacyl intermediates [19]. To confirm this hypothesis, the N162A protein was produced and characterized. Table 1 shows, as expected, that the mutation of N162 to alanine causes about a 200-fold lower dehydrogenase activity, together with a significant reduction in enzyme affinity for the substrate, especially for APAL. As the decrease in the activity rate is one or two orders of magnitude larger than the decline in affinity for the substrate, the result in Table 1 suggests that N162 is mainly involved in the catalytic activity of PsAMADH2.

Analysis of the betaine aldehyde dehydrogenase activity of PsAMADH2

The PsAMADH2 substrate channel consists of the same amino acid residues (W109, D110, D113, N162, Y163, L166, M167, W170, E260, F284, W288, I293, C294, S295, Q451, P452, C453 and W459) as the substrate

channel in the homology model of AMADH1 from maize (ZmAMADH1, GenBank accession GQ184593; data and model not shown). However, recombinant ZmAMADH1 (D. Kopečný *et al.*, unpublished results) is able to oxidize betaine aldehyde (BAL) as a substrate (K_m = 14 μM, V_{max} = 11 nmol·s^{-1}·mg^{-1}), whereas WT PsAMADH2 (K_m > 5 mM, V_{max} = 0.8 nmol·s^{-1}·mg^{-1}) and all of the mutated PsAMADH2 variants presented here cannot, except for the Y163A protein (K_m = 3.5 mM, V_{max} = 4.8 nmol·s^{-1}·mg^{-1}; Figs 4 and 5). This variant exhibits an unusual relative activity not only with BAL, but also with the synthetic quaternary ω-aminoaldehyde compounds *N*,*N*,*N*-trimethyl-3-aminopropionaldehyde (TMAPAL) and TMABAL (Fig. 5) (TMABAL possesses a longer carbon chain than TMAPAL). With respect to the fact that WT PsAMADH2 is capable of oxidizing TMABAL (see Figs 1 and 5), as is ZmAMADH1 (data not shown), the data in Fig. 5 on Y163A are even more puzzling. One possible explanation could perhaps be that the diameter of the middle section of the substrate channel near Y163 is the rate-limiting factor for BAL oxidation. It is possible that the Y163A mutation modifies (enlarges) this middle section in such a way that its altered shape resembles the shape and diameter of the corresponding section in ZmAMADH1. As a result, the bulkier side-chain of BAL fits the geometry of the Y163A substrate channel. This interpretation is consistent with the results on Y163 mentioned above, which suggest that Y163 affects the geometry of the substrate cavity (see Mutagenesis of aromatic amino acid residues in the PsAMADH2 substrate channel section). Taken together, the data in Fig. 5 indicate that the overall geometry of the PsAMADH2 active site, including the enlarged middle section, is more important for the betaine aldehyde dehydrogenase activity of PsAMADH2 than is the presence of the conserved Tyr side-chain in place of Y163 at the homologous position. This interesting aspect of AMADH deserves more attention in future research.

Conclusions

The high-resolution crystal structures of the two isoforms of PsAMADH [4] revealed several amino acid residues in their substrate channels that may be important for the high-affinity binding of ω-aminoaldehydes to AMADH and for the catalytic function of the enzyme. This work examines the consequences of mutagenic alterations of the substrate channel residues in PsAMADH2. The data presented here are consistent with the conclusion that the carboxylate residues D110 and D113 at the entrance to the substrate channel are essential for both the activity and substrate affinity of PsAMADH2, whereas N162, localized near the catalytic C294 residue, is important mainly for the catalytic rate of the enzyme. Inside the substrate cavity, the aromatic residues Y163 and W170, and, to some extent, L166 and M167 are necessary for the optimal overall geometry of the substrate channel that facilitates an appropriate orientation of the substrate towards C294, which in turn enables efficient oxidation. Moreover, the high K_m values of Y163A point to a hydrogen bonding interaction between the hydroxyl group of Y163 and the amino group of the substrate. In contrast, W288 probably preserves the diameter of the substrate channel without affecting the position of the substrate and, in turn, the catalytic rate of PsAMADH2. All of the results presented here provide experimental evidence that both substrate preference and binding are very complex in the plant AMADH family (family ALDH10).

Materials and methods

Site-directed mutagenesis of pea AMADH2

Site-directed mutants of the *PsMADH2* gene (1512 bp; EMBL/GenBank accession no. AJ315853) in the pCDFDuet vector were cloned using phosphorylated primers with the mutation at the 5′ end of one of them (tail to tail oriented), except for the W288A protein, which was prepared using two complementary primers containing the desired mutation (Table S1). The reaction mixture (50 μL) contained 5 μL of the Accuprime reaction buffer including deoxynucleoside triphosphates (dNTPs), 1 μL (~ 250 ng) of the dsDNA template, 1 μL (~ 100 pmol) of primers #1 and #2, and 1 μL of the Accuprime *Pfx* polymerase (Invitrogen, Carlsbad, CA, USA). The coding region was amplified using PCR in 30 cycles (cycle: denaturation at 94 °C for 40 s, annealing at 60 °C for 15 s, extension at 68 °C for 7 min). The *Dpn*I enzyme (Promega, Madison, WI, USA) was added to the reaction mixture and the mixture was incubated at 37 °C overnight. The PCR products for the other mutated proteins were incubated with *Dpn*I at 37 °C overnight, and then gel purified and ligated using the T4 DNA ligase (Promega), and finally transformed into NEB5-α competent *E. coli* cells (New England Biolabs, Hitchin, Hertfordshire, UK). The sequenced clones were transformed for expression in T7 express competent cells (New England Biolabs). Several clones for each mutated variant of PsAMADH2 were selected and then screened for expression by SDS/PAGE, western blot using HisProbe-HRP and activity assays. The work presented here is the first study to employ site-directed mutagenesis of PsAMADH2 residues based on findings obtained from the crystal structure of this enzyme [4]. Therefore, only mutagenic replacements with alanine were produced to

ensure significant impact of mutations on the active-site residues.

Enzyme purification, SDS/PAGE and identification

The mutated PsAMADH enzymes were produced as described for the WT enzyme [20]. All mutated proteins were purified using a column filled with cobalt(II)-charged IDA-Sepharose 6B (Sigma-Aldrich, Steinheim, Germany). SDS/PAGE used 4% stacking and 10% resolving polyacrylamide gels, and the separated proteins were visualized using Bio-Safe Coomassie Blue Stain (Bio-Rad, Hercules, CA, USA). The protein ladder 10–250 kDa (New England Biolabs) was used as a protein marker and the protein concentration was determined by the Bradford method [21]. The identity of the purified proteins and the presence of the desired mutations were confirmed by peptide mass fingerprinting (see Figs S1–S3), which followed SDS/PAGE and in-gel digestion [22].

Substrates and activity assays

Diethylacetals of APAL and ABAL, together with BAL chloride, were purchased from Sigma-Aldrich Chemie (Steinheim, Germany), as were the elementary aldehydes, pyridine carboxaldehydes and *N*,*N*-dimethyl-4-aminobutyraldehyde diethylacetal. Diethylacetals of GBAL and 3-guanidinopropionaldehyde (GPAL), and diethylacetal iodides of TMAPAL and TMABAL, were prepared synthetically [17,23]. Free aminoaldehydes were prepared by heating their acetals in a plugged test tube with 0.2 M HCl for 10 min [24]. The activity of the enzymes was measured spectrophotometrically by monitoring the formation of NADH (ε_{340} = 6.62 $mM^{-1} \cdot cm^{-1}$) at 37 °C. The reaction mixture in a cuvette contained 0.15 M Tris/HCl buffer, pH 9.0, 1 mM NAD^+ and appropriate amounts of AMADH. The enzyme reaction was initiated by the addition of the substrate at a final concentration of 1 mM. Kinetic constants were determined using GRAPHPAD PRISM 5.0 data analysis software (GraphPad Software, Inc., La Jolla, CA, USA).

CD spectroscopy

The far-UV CD spectra of WT PsAMADH2 and its mutated variants at a concentration of 0.5 $mg \cdot mL^{-1}$ in 20 mM Tris/HCl, pH 9.0, were recorded in the range 200–260 nm on a JASCO J-810 spectropolarimeter (JASCO Inc., Easton, MD, USA) using a 0.1-cm quartz cell. Each far-UV CD spectrum presented here is the average of three scans in order to obtain the optimal signal-to-noise ratio. After background subtraction and data smoothing, each CD signal was converted to the mean residual ellipticity $[\theta]'$. The relative contents of the secondary structural elements (α-helices, β-sheets) were determined using the K2d program [25].

Acknowledgements

This work was supported by grant nos. 522/08/0555 and P501/11/1591 from the Czech Science Foundation, grant no. MSM 6198959215 from the Ministry of Education, Youth and Sports of the Czech Republic and OP RD&I grant no. ED0007/01/01 (Centre of the Region Haná for Biotechnological and Agricultural Research). We thank Professor David Morris for his help with manuscript preparation, and Professor Milan Kodíček and Dr Zita Purkrtová (Department of Biochemistry and Microbiology, Institute of Chemical Technology, Prague, Czech Republic) for their assistance with CD measurements.

References

1 Yoda H, Hiroi Y & Sano H (2006) Polyamine oxidase is one of the key elements for oxidative burst to induce programmed cell death in tobacco cultured cells. *Plant Physiol* **142**, 193–206.

2 Šebela M, Frébort I, Petřivalský M & Peč P (2002) Copper/topa quinone-containing amine oxidases – recent research developments. In *Studies in Natural Products Chemistry*, Vol. **26** (Atta-ur-Rahman ed.), pp. 1259–1299. Elsevier, Amsterdam.

3 Li W, Yuan XM, Ivanova S, Tracey KJ, Eaton JW & Brunk UT (2003) 3-Aminopropanal, formed during cerebral ischaemia, is a potent lysosomotropic neurotoxin. *Biochem J* **371**, 429–436.

4 Tylichová M, Kopečný D, Moréra S, Briozzo P, Lenobel R, Snégaroff J & Šebela M (2010) Structural and functional characterization of plant aminoaldehyde dehydrogenase from *Pisum sativum* with a broad specificity for natural and synthetic aminoaldehydes. *J Mol Biol* **396**, 870–882.

5 Kirch HH, Bartels D, Wei Y, Schnable PS & Wood AJ (2004) The ALDH gene superfamily of *Arabidopsis*. *Trends Plant Sci* **9**, 371–377.

6 Bradbury LMT, Gillies SA, Brushett DJ, Waters DLE & Henry RJ (2008) Inactivation of an aminoaldehyde dehydrogenase is responsible for fragrance in rice. *Plant Mol Biol* **68**, 439–449.

7 Chen S, Yang Y, Shi W, Ji Q, He F, Zhang Z, Cheng Z, Liu X & Xu M (2008) Badh2, encoding betaine aldehyde dehydrogenase, inhibits the biosynthesis of 2-acetyl-1-pyrroline, a major component in rice fragrance. *Plant Cell* **20**, 1850–1861.

8 Wymore T, Hempel J, Cho SS, Mackerell AD Jr, Nicholas HB Jr & Deerfield DW II (2004) Molecular recognition of aldehydes by aldehyde dehydrogenase

and mechanism of nucleophile activation. *Proteins* **57**, 758–771.
9 Farrés J, Wang TT, Cunningham SJ & Weiner H (1995) Investigation of the active site cysteine residue of rat liver mitochondrial aldehyde dehydrogenase by site-directed mutagenesis. *Biochemistry* **34**, 2592–2598.
10 Perez-Miller SJ & Hurley TD (2003) Coenzyme isomerization is integral to catalysis in aldehyde dehydrogenase. *Biochemistry* **42**, 7100–7109.
11 Wang X & Weiner H (1995) Involvement of glutamate 268 in the active site of human liver mitochondrial (class 2) aldehyde dehydrogenase as probed by site-directed mutagenesis. *Biochemistry* **34**, 237–243.
12 Mann CJ & Weiner H (1999) Differences in the roles of conserved glutamic acid residues in the active site of human class 3 and class 2 aldehyde dehydrogenases. *Protein Sci* **8**, 1922–1929.
13 Ho BK & Gruswitz F (2008) HOLLOW: generating accurate representations of channel and interior surfaces in molecular structures. *BMC Struct Biol* **8**, 49.
14 Sugiyama S, Vassylyev DG, Matsushima M, Kashiwagi K, Igarashi K & Morikawa K (1996) Crystal structure of PotD, the primary receptor of the polyamine transport system in *Escherichia coli*. *J Biol Chem* **271**, 9519–9525.
15 Vassylyev DG, Tomitori H, Kashiwagi K, Morikawa K & Igarashi K (1998) Crystal structure and mutational analysis of the *Escherichia coli* putrescine receptor. Structural basis for substrate specificity. *J Biol Chem* **273**, 17604–17609.
16 Binda C, Coda A, Angelini R, Federico R, Ascenzi P & Mattevi A (1999) A 30-Å-long U-shaped catalytic tunnel in the crystal structure of polyamine oxidase. *Structure* **7**, 265–276.
17 Brauner F, Šebela M, Snégaroff J, Peč P & Meunier JC (2003) Pea seedling aminoaldehyde dehydrogenase: primary structure and active site residues. *Plant Physiol Biochem* **41**, 1–10.
18 Wood PL, Khan MA & Moskal JR (2007) The concept of 'aldehyde load' in neurodegenerative mechanisms: cytotoxicity of the polyamine degradation products hydrogen peroxide, acrolein, 3-aminopropanal, 3-acetamidopropanal and 4-aminobutanal in a retinal ganglion cell line. *Brain Res* **1145**, 150–156.
19 Steinmetz CG, Xie P, Weiner H & Hurley TD (1997) Structure of mitochondrial aldehyde dehydrogenase: the genetic component of ethanol aversion. *Structure* **5**, 701–711.
20 Tylichová M, Briozzo P, Kopečný D, Ferrero J, Moréra S, Joly N, Snégaroff J & Šebela M (2008) Purification, crystallization and preliminary crystallographic study of a recombinant plant aminoaldehyde dehydrogenase from *Pisum sativum*. *Acta Crystallogr Sect F: Struct Biol Cryst Commun* **64**, 88–90.
21 Bradford MM (1976) A rapid and sensitive method for the quantitation of microgram quantities of protein utilizing the principle of protein–dye binding. *Anal Biochem* **72**, 248–254.
22 Šebela M, Štosová T, Havliš J, Wielsch N, Thomas H, Zdráhal Z & Shevchenko A (2006) Thermostable trypsin conjugates for high-throughput proteomics: synthesis and performance evaluation. *Proteomics* **6**, 2959–2963.
23 Vaz FM, Fouchier SW, Ofman R, Sommer M & Wanders RJA (2000) Molecular and biochemical characterization of rat γ-trimethylaminobutyraldehyde dehydrogenase and evidence for the involvement of human aldehyde dehydrogenase 9 in carnitine biosynthesis. *J Biol Chem* **275**, 7390–7394.
24 Trossat C, Rathinasabapathi B & Hanson AD (1997) Transgenically expressed betaine aldehyde dehydrogenase efficiently catalyzes oxidation of dimethylsulfoniopropionaldehyde and ω-aminoaldehydes. *Plant Physiol* **113**, 1457–1461.
25 Andrade MA, Chacon P, Merelo JJ & Moran F (1993) Evaluation of secondary structure of proteins from UV circular dichroism spectra using an unsupervised learning neural network. *Protein Eng* **6**, 383–390.

Supporting information

The following supplementary material is available:
Fig. S1. Matrix-assisted laser desorption ionization-time of flight (MALDI-TOF) peptide mass fingerprinting – a comparison of differences between wild-type (WT) PsAMADH2 and the mutated proteins E106A, D110A, D113A, D110A + D113A and E106A + D110A + D113A on the peptide level.
Fig. S2. Matrix-assisted laser desorption ionization-time of flight (MALDI-TOF) peptide mass fingerprinting of the mutated proteins W109A and W288A.
Fig. S3. Matrix-assisted laser desorption ionization-time of flight (MALDI-TOF) peptide mass fingerprinting of the mutated proteins C453A, W170A, Y163A, L166Q + M167I and N162A.
Fig. S4. Activity of wild-type (WT) PsAMADH2 in 150 mM glycine–NaOH buffer in the pH range 8.8–10.4.
Table S1. Primer pairs used for site-directed mutagenesis of PsAMADH2.

This supplementary material can be found in the online version of this article.

Please note: As a service to our authors and readers, this journal provides supporting information supplied by the authors. Such materials are peer-reviewed and may be re-organized for online delivery, but are not copy-edited or typeset. Technical support issues arising from supporting information (other than missing files) should be addressed to the authors.